Available online at www.sciencedirect.com
ScienceDirect
Journal of Magnetism and Magnetic Materials 306 (2006) 30–34
www.elsevier.com/locate/jmmm

Synthesis and magnetic characterization of magnetite particles embedded in mesoporous MCM-41

Nicolás A. Fellenz[a], Sergio G. Marchetti[a,*], José F. Bengoa[a], Roberto C. Mercader[b], Silvana J. Stewart[b]

[a]*Departamento de Química, Facultad de Ciencias Exactas, Universidad Nacional de La Plata, CONICET, CINDECA, CICPBA, 47 No 257, 1900 La Plata, Argentina*
[b]*Departamento de Física, Facultad de Ciencias Exactas, Universidad Nacional de La Plata, IFLP-CONICET, C.C. 67, 1900 La Plata, Argentina*

Received 28 October 2005; received in revised form 9 February 2006
Available online 10 March 2006

Abstract

A solid of 7.7 wt% iron-loaded MCM-41 was obtained by impregnating the mesoporous material with an Fe-carrying organic salt after subjecting the matrix to a silylation treatment. The Mössbauer and magnetic results show that the as-prepared composite is mainly made up of fine Fe_3O_4 particles that display a superparamagnetic relaxation at room temperature and block at $\approx$42 K. A percentage of $\approx$24% of the iron-containing phases is magnetically blocked at room temperature, and belongs to Fe_3O_4 that undergoes the Verwey transition. In addition, there is a minor Fe(III) phase that remains paramagnetic down to 4.2 K.

PACS: 75.30.Cr; 75.50.Tt; 75.60.Ej

Keywords: Magnetically ordered materials; Nanostructures; Chemical synthesis; Nanofabrications; Magnetic nanoarrays synthesis; Fe_3O_4; MCM-41; Nanoparticles magnetism; Silylated MCM-41

1. Introduction

The search for methods to produce one-dimensional magnetic arrays has attracted much attention because of their potential applications in high-density magnetic recording media and other nanodevices [1]. Nanowires with specific physical properties have been synthesized by several methods like laser ablation [2], electrodeposition [3] or supercritical fluid phase inclusion [4] techniques. These processes, however, have the common disadvantage of their complexity.

Highly ordered mesoporous materials like MCM-41 can be used as templates to confine conveniently magnetic compounds [5,6] in a quasi-one-dimensional array because of its particular topology of regular hexagonal parallel channels with usual average diameters of less than 5 nm. In spite of the advantage that the high surface area of MCM-41 offers for many applications, the irregular coating of its channels with silanol groups hinders the uniform filling of the pores. In previous works [7,8], we have showed that hematite (α-Fe_2O_3) fills non-homogeneously the MCM-41 pores after impregnation by incipient wetness with an aqueous solution of iron nitrate.

To promote the pore filling and obtain quasi-one-dimensional arrays of the magnetic Fe_3O_4 iron oxide, we have tried a new and straightforward route using an Fe-carrying organic salt after subjecting the support to a silylation treatment. Here we report the synthesis and characterization of a magnetite-loaded MCM-41 solid.

2. Experimental Section

Previous to the silylation treatment, MCM-41 of specific surface area of 940 m^2/g and average pore diameter of 2.8 nm was dehydrated by heating for 3 h at 573 K and $p_{vacuum} < 10^{-3}$ Torr. The silylation treatment was carried out with hexamethyl-disilazane (HMDS) in toluene

*Corresponding author. Tel.: +54 221 4210711; fax: +54 221 4211353.
E-mail address: march@quimica.unlp.edu.ar (S.G. Marchetti).

0304-8853/$ - see front matter © 2006 Elsevier B.V. All rights reserved.
doi:10.1016/j.jmmm.2006.02.101

(0.05 M) inside a glove box in N_2 atmosphere. This solution was added to the dehydrated MCM-41 (20 cm^3/g solid). The mixture was heated at 393 K for 90 min with stirring. Then it was filtrated and washed with toluene to eliminate the HMDS excess. Finally, the solid was dried in an oven at 333 K for 16 h and impregnated with the $Fe(AcAc)_3$ solution in benzene with a concentration enough to produce an iron loading of about 5 wt%. After impregnation, the solid was heated at 13 K/min from room temperature to 683 K and annealed at this temperature in a closed vessel for 20 h. In previous assessments these had proved to be the optimal preparation conditions to decompose bulk $Fe(AcAc)_3$ into Fe_3O_4.

The resulting composite was characterized by X-ray diffraction (XRD) (Cu Kα radiation) and atomic absorption spectroscopy. The Mössbauer spectra at 298 and 22 K were taken in transmission geometry with a constant acceleration spectrometer. A source of ^{57}Co in an Rh matrix of nominally 50 mCi was used. The isomer shifts, δ, were calibrated against a metallic α-Fe foil at room temperature. The temperature between 22 and 298 K was varied using a Displex DE-202 closed cycle cryogenic system. The 4.2 K Mössbauer spectrum was taken, using a sinusoidal velocity waveform in a cryostat, where both the source and the sample were held at liquid helium temperature. The magnetization vs. magnetic field (M–H) measurements recorded at 5 and 300 K were carried out using a commercial superconducting quantum interference device magnetometer. The AC susceptibility measurements between 13 and 325 K were taken in a Lake Shore 7130 susceptometer using an exciting field amplitude of 1 Oe and a frequency of 825 Hz.

3. Results and discussion

The XRD patterns of MCM-41 and the composite are displayed in Fig. 1. The intense peak of the (1 0 0) reflection at $2\theta = 2.1^\circ$ is indicative that the structure of the hexagonal ordered mesoporous solid MCM-41 was preserved over the preparation process. The iron loading, determined by atomic absorption spectroscopy, was 7.7 wt%. No change in the position of the (1 0 0) peak was observed after the iron loading.

The Mössbauer spectra are shown in Fig. 2. The room temperature spectrum is composed of a resolved magnetic signal (relative area $\approx$24%) and a central doublet. This spectrum was best-fitted to two sextets and a Fe^{3+} doublet, respectively. The hyperfine parameters obtained for the magnetic signal indicates that it belongs to Fe_3O_4 [9] (Table 1). When the temperature decreases, the area of the magnetic signal increases and the background buckles. At 22 K a relaxing component also had to be included in the fitting. Finally, at 4.2 K the relative area of the doublet decreases down to 12% at the expense of the magnetic components. At no temperature a signal belonging to metallic iron was found within the statistical uncertainty.

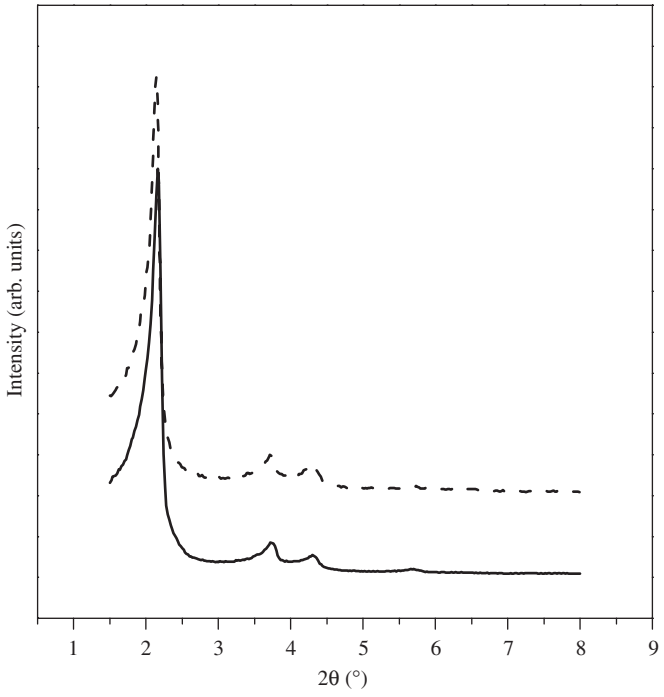

Fig. 1. XRD patterns of the MCM-41 hexagonal ordered mesoporous solid (solid line), and the composite after iron loading and calcinations (dashed line).

Considering that surface effects are expected to take place because of the reduced pore diameters of the channels for those iron species embedded in the MCM-41 matrix, we assign the distributed signal at 4.2 K, to Fe atoms located at the surface of these species (Table 1). Their individual magnetic moments would be arranged in a partially randomly frozen way, as in a spin-glass-like state. On the other hand, the presence of a doublet at 4.2 K indicates the existence of a paramagnetic fraction. Taking into account that the silylation treatment neutralizes the existing surface silanol groups, the assignment of this paramagnetic species to Fe^{3+} ions in the silicate framework [10] may be discarded. This signal arises more likely from isolated Fe–O–Fe entities covering the MCM-41 pore walls.

The M–H hysteresis loops are shown in Fig. 3. The magnetization values are normalized to the Fe_3O_4 content, assuming that all the iron atoms in the sample are forming this phase. At 300 K the loop shows a rapid increase of the magnetization at lower fields (up to $\approx$2 kOe) and then attains a linear behavior without reaching the complete saturation for fields up to 50 kOe. The high-field susceptibility, χ_H, taken from the slope of this linear region is $\chi_H \approx 2.5 \times 10^{-5}$ emu g^{-1} Oe^{-1}. A saturation magnetization $M_s = 20$ emu/g of Fe_3O_4 was estimated assuming for the high-field region a $M(H)$ dependence of the form $M = M_s(1 - \alpha/H)$, where α is a fitting parameter.

The cycle also shows hysteresis, which is compatible with the ferrimagnetic nature of magnetite. The coercive field is $H_C = 80$ Oe and the remanence $M_r = 3.1$ emu/g. At $T =$ 5 K the hysteresis cycle shows an increase of the magnetic

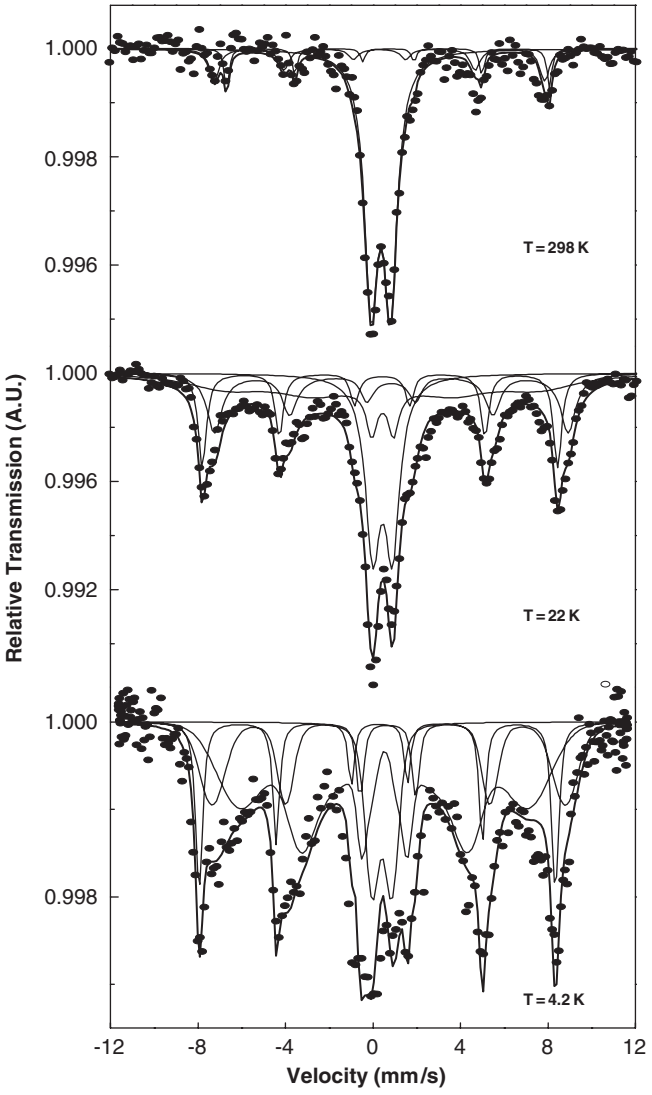

Fig. 2. Mössbauer spectra at 298, 22 and 4.2 K. The solid lines are the results of the fitting procedure described in the text.

area with hysteresis parameters $H_C = 530\,\text{Oe}$, $M_s = 30\,\text{emu/g}$ and $M_r = 8.3\,\text{emu/g}$. We observe that the M_s value is noticeably low in comparison to the M_s typically reported for bulk Fe_3O_4 (85–100 emu/g). However, such M_s reduced values have been also reported for nanostructured magnetite and ascribed to the spin disorder at the surface [11,12]. This explanation is in agreement with the previous assignment of our broad Mössbauer sextet to surface iron species. On the other hand, the M_r/M_s ratio, 0.28 at 5 K, is lower than the 0.5 value predicted for non-interacting uniaxial nanoparticles [13]. This is probably due to the presence of particle interactions. Taking into account the magnetic area of the hysteresis loop at 5 K, we estimate an effective anisotropy constant $K_{\text{eff}} = 2.4 \times 10^4\,\text{erg/cm}^3$ for the magnetite particles similarly to previously reported Fe_3O_4 nanoparticle systems [11,14].

At 5 K the magnetization does not saturate and χ_H has increased by one order of magnitude with respect to the χ_H value at 300 K. A lack of saturation is usually observed in ferrimagnetic nanoparticles due to the spin canting at the particle surface layer. However, the thermal dependence of χ_H indicates that for the current system it is mainly related to the presence of a paramagnetic phase, in agreement with the Mössbauer results.

Fig. 4 shows the results of the susceptibility measurements. On decreasing the temperature the in-phase component, χ', monotonically decreases down to 110 K where a discontinuity is clearly observed. This change of slope corresponds to the Verwey transition temperature of Fe_3O_4, through which the net magnetic moment decreases because the antiferromagnetic exchange interaction between the hopping electrons and the inner electrons at iron cation octahedral sites becomes dominant when the thermal energy decreases [15]. In addition, χ' shows a shoulder near 50 K. More clearly, the out-of-phase susceptibility component, χ'', directly associated to the magnetic energy dissipation, displays a maximum at 42 K (see the inset in Fig. 4).

An anomaly in χ' near 50 K has also been observed in microsized Fe_3O_4 which, although related to relaxation processes, is still not fully understood [15]. Zhang et al. [16] have observed a maximum at ≈ 50 K in the thermal dependence of the magnetization in Fe_3O_4 nanowires prepared by electro-deposition into anodic alumina templates with pore diameters of 200 nm. This was interpreted as the Verwey transition of Fe_3O_4 taking place at a lower temperature than bulk Fe_3O_4 ($T_V \approx 110-120$ K) as a consequence of the reduced dimension of the array. A considerable shift of the Verwey transition temperature to lower values has also been observed for Fe_3O_4 nanoparticles of sizes ≈ 20 nm [11]. In our case, those particles included within the MCM-41 channels would exhibit a shift of the Verwey transition, but, considering also our Mössbauer results, we believe rather that the shoulder of χ' at 50 K and the χ'' maximum at 42 K are probably associated to the blocking of the magnetic moments of the smaller Fe_3O_4 particles.

Based on the above results, a possible interpretation of the synthesis process and the structure of the composite could be as follows. Because the inner walls of the MCM-41 channels are irregularly coated with isolated surface silanol groups [17], hydrophobic and hydrophilic areas exist within the channels. Hence, when an inorganic iron salt in a polar solvent is used at the impregnation step, an heterogeneous distribution of the iron product is obtained in the final composite [7,8]. If an organometallic iron salt in a non-polar solvent is used instead, the distribution of the solution inside the pores will be the reverse of the polar solution case, but at the end an inhomogeneous filling will inevitably occur. Thus, to produce a complete homogeneously hydrophobic surface that ensures an even Fe_3O_4 distribution within the MCM-41 channels, we neutralized the silanol groups with a silylation agent. This treatment would ensure that the iron species "spread" over the surface of the MCM-41 channels after impregnation.

Table 1
Hyperfine parameters yielded by fitting the Mössbauer spectra at the indicated temperatures as described in the text

Species	Parameters	$T = 298$ K	$T = 22$ K	$T = 4.2$ K
Fe in site A	H (T)	46.8±0.6	50.4±0.1	50.5±0.2
	δ (mm/s)	0.3 ([a])	0.37±0.03	0.24±0.02 ([b])
	2ε (mm/s)	0 ([a])	–0.10±0.04	–0.10±0.05
	Relative area (%)	15±7	18±7	15±2
Fe in site B	H (T)	45.8±0.3	50.3±0.4	50.1±0.5
	δ (mm/s)	0.70±0.05	0.84±0.08	0.7 ([a]) ([b])
	2ε (mm/s)	–0.02±0.08	0 ([a])	0.1±0.1
	Relative area (%)	9±5	23±9	20±2
Relaxing signal	$<H$ (T)$>$	—	50 ([a])	—
	δ (mm/s)	—	0.4±0.1	—
	2ε (mm/s)	—	0 ([a])	—
	Relative area (%)	—	31±10	
Distributed signal	$<H$ (T)$>$	—	—	34.6
	δ (mm/s)	—	—	0.52±0.08 ([b])
	2ε (mm/s)	—	—	–0.1±0.1
	Relative area (%)		—	53±2
Superparamagnetic or paramagnetic Fe^{3+} signal	Δ (mm/s)	0.88±0.02	0.9±0.1	0.9 ([a])
	δ (mm/s)	0.36±0.02	0.44±0.05	0.41±0.06 ([b])
	Relative area (%)	76±3	28±2	12±1

$<$H$>$: Average hyperfine field.
(a) Parameter held fixed while fitting.
(b) At 4.2 K sample and source are at the same temperature.
Isomer shifts are referred to α-Fe at room temperature.

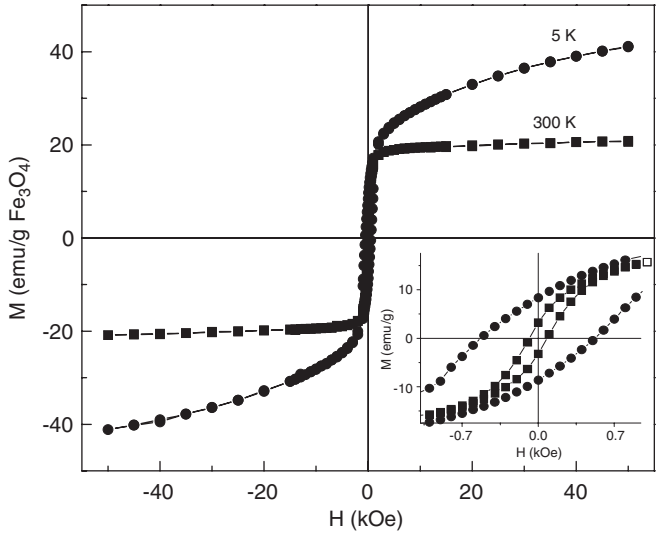

Fig. 3. Hysteresis cycles at 5 and 300 K using a maximum applied magnetic field $H = 50$ kOe. The inset shows the low-field regions of the cycles.

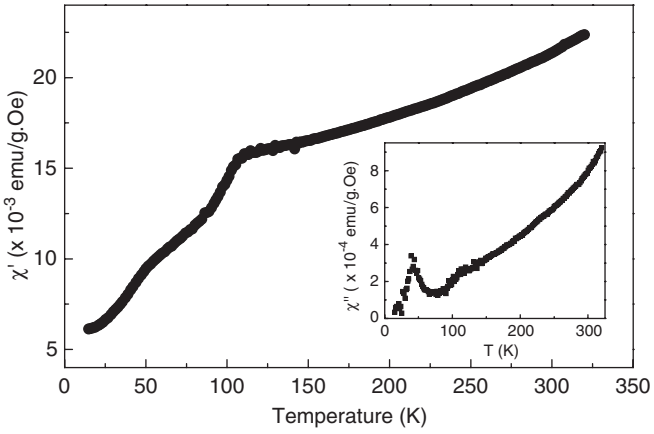

Fig. 4. In-phase AC susceptibility (χ′), measured with a frequency of 825 Hz and amplitude of 1 Oe. Inset: Out-of-phase component (χ″). The data are normalized to the Fe_3O_4 content.

A major percentage of these species agglomerate into very fine Fe_3O_4 particles that relax superparamagnetically at room temperature and progressively block. The fraction that does not cluster keeps on covering the inner surface in the form of a monolayer of Fe-O-Fe entities that give rise to the paramagnetic signal in the Mössbauer spectrum at 4.2 K and are also revealed by the magnetization results.

The remaining percentage of iron oxides forms bigger Fe_3O_4 particles that display a blocked Mössbauer signal at room temperature. This fraction brings about the hysteresis observed in the M–H curve and probably undergoes the observed Verwey transition at the temperature $T_V = 110$ K. Such coexistence of a ferrimagnetic iron oxide phase (blocked or in a superparamagnetic state) and a paramagnetic Fe^{3+} phase has also been obtained in other iron-containing MCM-41 silicates prepared by

different procedures [5,10], and has been attributed to a scarce ill-formed phase.

4. Conclusions

The impregnation of MCM-41 with a solution of $Fe(AcAc)_3$ in benzene after subjecting the matrix to a silylation treatment has produced a 7.7 wt% iron-loaded solid. The subsequent annealing has successfully brought about MCM-41 containing Fe_3O_4 and a small paramagnetic fraction of isolated Fe–O–Fe entities. Magnetic and hyperfine results allow concluding that the magnetite is composed of a high percentage of small particles that relax superparamagnetically and a minor fraction of large particles in a blocked magnetic state.

Ackowledgment

We thank R. B. Scorzelli, I. Souza-Acevedo and A. Caytuero, for the 4.2 K Mössbauer measurement. SGM, SJS and RCM thank CONICET, Argentina, for partial financial support (PIP2853 and PICT 14-11267).

References

[1] Q.A. Pankhurst, R.J. Pollard, J. Phys.: Condens. Matter. 5 (1993) 8487.
[2] A.M. Morales, C.M. Lieber, Science 279 (1998) 208.
[3] M. Lederman, R. O'Barr, S. Schultz, Trans. Magn. 31 (1995) 3793.
[4] T.A. Crowley, K.J. Ziegler, D.M. Lyons, D. Erts, H. Olin, M.A. Morris, J.D. Holmes, Chem. Mater. 15 (2003) 3518.
[5] S. Liu, Q. Wang, P. Van der Boort, P. Cool, E.F. Vansant, M. Jiang, J. Magn. Magn. Mater. 280 (2004) 31.
[6] J.S. Jung, K.H. Choi, W.S. Chae, Y.R. Kim, J.H. Jun, L. Malkinski, T. Kodenkandath, W. Zhou, J.B. Wiley, C.J. O'Connor, J. Phys. Chem. Solids 64 (2003) 385.
[7] J.F. Bengoa, M.V. Cagnoli, N.G. Gallegos, A.M. Alvarez, L.V. Mogni, M.S. Moreno, S.G. Marchetti, Micropor. Mesopor. Mater. 84 (2005) 153.
[8] M.V. Cagnoli, N.G. Gallegos, J.F. Bengoa, A.M. Alvarez, M.S. Moreno, A. Roig, S.G. Marchetti, R.C. Mercader, Am. Inst. Phys. Conf. Proc. 765 (2005) 13.
[9] R.E. Vandenberghe, E. De Grave, C. Landuydt, L.H. Bowen, Hyperfine Interact 53 (1990) 175.
[10] P. Selvam, S.E. Dapurkar, S.K. Badamali, M. Murugasan, H. Kuwano, Catal. Today 68 (2001) 69.
[11] G.F. Goya, T.S. Berquo, F.C. Fonseca, M.P. Morales, J. Appl. Phys. 94 (2003) 3520.
[12] R.V. Kumar, Y. Koltypin, Y.S. Cohen, Y. Cohen, D. Aurbach, O. Palchik, I. Felner, A. Gedanken, J. Mater. Chem. 10 (2000) 1125.
[13] B.D. Cullity, Introduction to Magnetic Materials, Addison-Wesley, Reading, MA, 1972.
[14] W. Luo, S.R. Nagel, T.F. Rosenbaum, R.E. Rosensweig, Phys. Rev. Lett. 67 (1991) 2721.
[15] A.R. Muxworthy, E. McClelland, Geophys. J. Int. 140 (2000) 101.
[16] L.Y. Zhang, D.S. Xue, X.F. Xu, A.B. Gui, C.X. Gao, J. Phys. Condens. Matter 16 (2004) 4541.
[17] A. Jentys, K. Kleestorfer, H. Vinek, Micropor. Mesopor. Mater. 27 (1999) 321.